

A modified SMAC scheme for a non-equilibrium compressible two-phase fluid

H. Y. Yoon, J. J. Jeong

Korea Atomic Energy Research Institute, 1045 Daedeok-daero, Yuseong-gu, Daejeon, 305-353, Korea,
hyyoon@kaeri.re.kr

1. Introduction

Two-phase flows appear in LWRs (light water reactors) in highly complex forms depending on their thermal-hydraulic conditions. System codes have mainly been providing the performance and safety analysis of these complex two-phase phenomena during anticipated transients or accidents. More sophisticated two-phase computational models are needed for a detailed analysis of LWR components such as a reactor vessel core, downcomer, steam generators, etc., enabling more operational margins.

In many fluid flow calculations, there are efficient numerical methods like SMAC [1], ICE [2] and SIMPLE [3] where the mass fluxes from the momentum equation are solved using an assumed pressure field, and the pressure field is corrected based on a continuity. The ICE is similar to SMAC except it can be applied to compressible fluids. SMAC and SIMPLE differ in their degree of implicitness. In all these methods, the energy equations are solved using the mass flux and the pressure from the momentum and continuity equations. However, the pressure fields in a two-phase flow need to be corrected based on energy equation as well as continuity when their thermo-dynamic states are far from an equilibrium state.

In this paper, the SMAC method is modified for an application to non-equilibrium two-phase flow, where the phase change term appearing in the continuity equation is implemented in an implicit way for the pressure correction calculation. The compressibility is also considered. The present method is compared to a method [4], where the energy and continuity equations are coupled simultaneously during the pressure correction step.

2. Governing Equations

The two-phase governing equations are employed for the transient two-phase analysis. The continuity, momentum, and energy equations are;

$$\frac{\partial}{\partial t}(\alpha_k \rho_k) + \nabla \cdot (\alpha_k \rho_k \underline{u}_k) = \Gamma_k \quad (1)$$

$$\frac{\partial}{\partial t}(\alpha_k \rho_k \underline{u}_k) + \nabla \cdot (\alpha_k \rho_k \underline{u}_k \underline{u}_k) = -\alpha_k \nabla P + \nabla \cdot [\alpha_k \underline{\tau}_k] \quad (2)$$

$$+ \alpha_k \rho_k \underline{g} + P \nabla \alpha_k + M_k^{mass} + M_k^{drag} + M_k^{VM}$$

$$\frac{\partial}{\partial t}[\alpha_k \rho_k e_k] + \nabla \cdot (\alpha_k \rho_k e_k \underline{u}_k) = -\nabla \cdot (\alpha_k q_k) \quad (3)$$

$$+ \nabla \alpha_k \underline{\tau}_k : \nabla \underline{u}_k - P \frac{\partial}{\partial t} \alpha_k - P \nabla \cdot (\alpha_k \underline{u}_k) + I_k + Q_k$$

where α_k , ρ_k , \underline{u}_k , P_k , and Γ_k are the k-phase volume fraction, density, velocity, pressure, and interface mass transfer rate, respectively. M_k represents the interfacial momentum transfer due to the mass exchange, the drag, and the virtual mass.

3. Modified SMAC Scheme

At first, the momentum equations are explicitly solved to obtain temporal phasic velocities, \bar{u}_k^* , at cell center by

$$\bar{u}_k^* = a_k \nabla p^n + \bar{s}_k, \quad (4)$$

where the terms in the right hand side are known values at the old time step. Phasic velocities at new time step, \bar{u}_k^{n+1} , corresponding to the pressure p^{n+1} can be written as

$$\bar{u}_k^{n+1} = a_k \nabla p^{n+1} + \bar{s}_k. \quad (5)$$

Subtracting Eq. (4) from Eq. (5) and then taking divergence,

$$\nabla \cdot \bar{u}_k^{n+1} = a_k \nabla^2 p^{n+1} + \nabla \cdot \bar{u}_k^*, \quad (6)$$

where $p' = p^{n+1} - p^n$ and $\nabla \cdot \bar{u}_k^{n+1}$ is removed using the continuity in the SMAC. For example, it is zero for an incompressible fluid. For a two-phase flow where phase change occurs, the energy as well as continuity equations need to be coupled for the elimination of $\nabla \cdot \bar{u}_k^{n+1}$. Solving the pressure matrix from Eq. (6) takes a major portion of the calculation time. To make the pressure matrix symmetric, the phase change and transient terms in the continuity equation are implicitly computed rather than coupling the energy and continuity equations. Phasic continuity equation can be written as

$$\frac{\partial \alpha_k}{\partial t} + \frac{\alpha_k}{\rho_k} \left(\frac{\partial \rho_k}{\partial t} + \bar{u}_k \cdot \nabla \rho_k \right) + \nabla \cdot (\alpha_k \bar{u}_k) = \frac{\Gamma_k}{\rho_k}, \quad (7)$$

where Γ_k is a volumetric mass transfer rate accounting for a phase change. For a steam it is defined as

$$\Gamma_v = - \frac{H_{iv}(T^s - T_v) + H_{il}(T^s - T_l)}{h_v^* - h_l^*}, \quad (8)$$

where $(h_v^*, h_l^*) = (h_v^s, h_l^s)$; $\Gamma_v \geq 0$, $(h_v^*, h_l^*) = (h_v, h_l^s)$; $\Gamma_v < 0$. The second term in the left hand side of Eq.(7) is approximated as

$$\left(\frac{\partial \rho_k}{\partial t} + \bar{u}_k \cdot \nabla \rho_k \right) = \frac{\partial \rho_k}{\partial t} = \left(\frac{\partial \rho_k}{\partial p} \right) \frac{\partial p}{\partial t}, \quad (9)$$

assuming that the speed of sound is much faster than that of the fluid. Eq. (8) is linearized in an implicit form

$$\Gamma_v^{n+1} = - \frac{H_{iv}}{h_v^* - h_l^*} \left(\left(\frac{dT^s}{dp} \right)_i^n - \left(\frac{\partial T_v}{\partial p} \right)_i^n \right) p'$$

$$-\frac{H_{il}}{h_v^* - h_l^*} \left(\left(\frac{dT^s}{dp} \right)_i^n - \left(\frac{\partial T_l}{\partial p} \right)_i^n \right) p' - \frac{H_{iv}}{h_v^* - h_l^*} (T_i^{s,n} - T_{v,i}^n) - \frac{H_{il}}{h_v^* - h_l^*} (T_i^{s,n} - T_{l,i}^n) \quad (10)$$

4. Numerical Results

For the verification of the numerical scheme, a boiling flow in a two-dimensional vertical pipe of 0.1 m in diameter and 2 m in height was simulated. Figure 1 shows the grid and void fraction profile at a steady state. A volumetric heat source was imposed for the whole pipe, which was linearly increased from 0 MW/m³ to 20.0 MW/m³ during the first 10 seconds and then kept constant. Initially, the flow in the pipe was stagnant and subcooled water of 450.0 K was introduced to the inlet at a constant velocity of 0.1 m/s. The exit pressure was maintained at 1.0 MPa. A null transient calculation was conducted to reach a steady state.

Figure 2 shows similar axial void fraction profiles by the modified SMAC and a coupled scheme after the steady state was reached. The void fraction was averaged over the x-direction. Figure 3 compares the CPU time of both schemes when the number of cell varies from 500 to 10⁵. Explicit calculation time is the same for each scheme as indicated by the triangles. The pressure matrix solver of the modified SMAC scheme is faster than that of the coupled scheme. The difference becomes significant as the number of cell increases.

5. Conclusions

A modified SMAC scheme was proposed for a non-equilibrium two-phase flow. Compressibility has also been considered. The calculations are stable by treating the phase change and transient terms implicitly. Two-dimensional boiling flow was successfully calculated using the present method, and the results were very close to that of the coupled scheme. The modified SMAC scheme has an advantage in its calculation time, especially when the number of cells is large, over the coupled scheme. When the degree of the non-equilibrium state is large such as a flashing, the calculation is hard to converge. In such cases, the coupled scheme is preferred.

REFERENCES

- [1] Amsden, A.A., and Harlow, F. H., "The SMAC Method: A Numerical Technique for Calculating Incompressible Flows," LA-4370, 1970.
- [2] Harlow, F. H., and Amsden, A.A., "A Numerical Fluid Dynamics Calculation Method at All Flow Speeds," J. Comput. Phys. 8, 197-213, 1971.
- [3] Patankar, Suhas V., "Numerical Heat and Mass Transfer," Hemisphere Pub. Co., 1980.
- [4] Jeong, J. J., et al., "A Semi-implicit numerical for a transient two-fluid three-field model on an unstructured

grid," Int. Comm. Heat Mass Transfer, to be published, 2008.

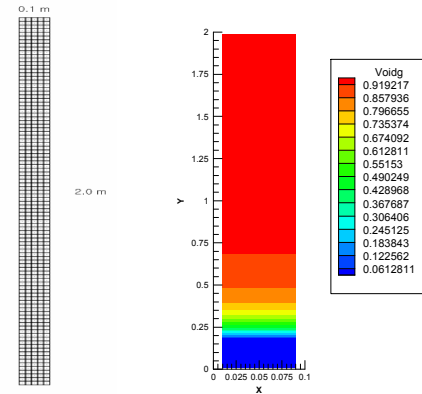


Figure 1. Boiling in a 2D vertical pipe

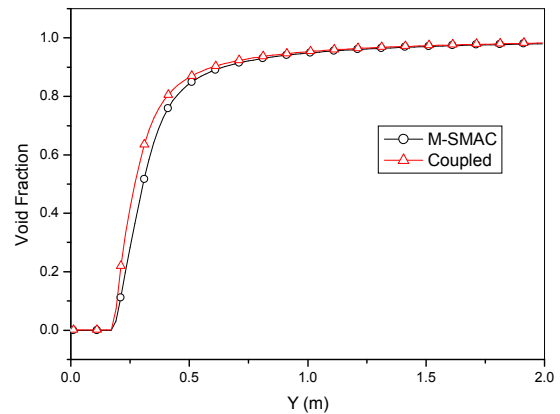


Figure 2. Comparison of the axial void fraction

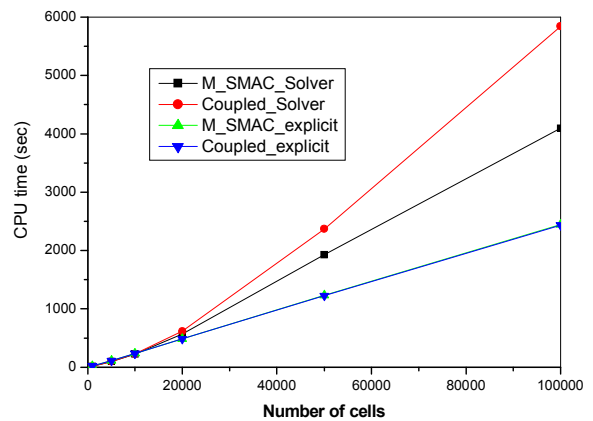


Figure 3. CPU time versus the number of cells